Beta-induced Alfvén-acoustic eigenmodes in National Spherical Torus Experiment and DIII-D driven by beam ions[a)]

N. N. Gorelenkov,[1,b)] M. A. Van Zeeland,[2] H. L. Berk,[3] N. A. Crocker,[4] D. Darrow,[1] E. Fredrickson,[1] G.-Y. Fu,[1] W. W. Heidbrink,[5] J. Menard,[1] and R. Nazikian[1]
[1]*Princeton Plasma Physics Laboratory, Princeton University, Princeton, New Jersey 08543, USA*
[2]*General Atomics, San Diego, California 92186, USA*
[3]*Institute for Fusion Studies, University of Texas, Austin, Texas 78712, USA*
[4]*Institute of Plasma and Fusion Research, University of California, Los Angeles, California 90095, USA*
[5]*University of California, Irvine, California 92697, USA*

(Received 7 December 2008; accepted 16 February 2009; published online 1 April 2009)

Kinetic theory and experimental observations of a special class of energetic particle driven instabilities called here beta-induced Alfvén-acoustic eigenmodes (BAAEs) are reported confirming, previous results [N. N. Gorelenkov *et al.*, Plasma Phys. Controlled Fusion **49**, B371 (2007)]. The kinetic theory is based on the ballooning dispersion relation where the drift frequency effects are retained. BAAE gaps are recovered in kinetic theory. It is shown that the observed certain low-frequency instabilities on DIII-D [J. L. Luxon, Nucl. Fusion **42**, 614 (2002)] and National Spherical Torus Experiment [M. Ono, S. M. Kaye, Y.-K. M. Peng *et al.*, Nucl. Fusion **40**, 557 (2000)] are consistent with their identification as BAAEs. BAAEs deteriorate the fast ion confinement in DIII-D and can have a similar effect in next-step fusion plasmas, especially if excited together with multiple global toroidicity-induced shear Alfvén eigenmode instabilities. BAAEs can also be used to diagnose safety factor profiles, a technique known as magnetohydrodynamic spectroscopy. © *2009 American Institute of Physics*.
[DOI: 10.1063/1.3097920]

I. INTRODUCTION

Low-frequency plasma oscillations due to coupling of two fundamental magnetohydrodynamic (MHD) branches, Alfvénic and acoustic, have attracted a lot of interest in recent years. One solution, the geodesic acoustic mode (GAM), is known to be a part of the turbulent processes.[1] Another class of global modes is responsible for the instabilities driven by energetic particles in tokamak plasmas such as beta-induced Alfvén and Alfvén-acoustic eigenmodes [BAE[2] and BAAE,[3] respectively]. These modes can have deleterious effects on plasma performance arising from the induced fast ion loss and wall heat load. Because of their very low frequencies near the rational surface and their global mode structure, BAAEs can potentially participate in background plasma turbulence and in the generation of the zonal flows. One positive aspect of these modes is that BAAEs in particular can be used for so-called MHD spectroscopy to diagnose plasma parameters such as the safety factor profiles, which is especially important in the burning plasma conditions where measurements of the internal safety factor profile will be difficult.

Interacting Alfvén-acoustic branches and resulting gap structures have been reported earlier using analytical theory[4] and numerical simulations.[5] However, global modes localized to the BAAE continuum extremum points have been found only recently.[3] Notably the search for the low-frequency modes inside the wider BAE gap with the antenna code did not result in the BAAE modes[5] because of their strong radial localization and thus weak coupling to the edge. Instead, a more global BAE-like plasma response was found with a strong characteristic interaction with the continuum.

To illustrate the toroidicity effect on the MHD continuum we first consider ideal MHD Alfvénic and acoustic branches in a cylinder. In this case these two waves do not interact and their solutions are uncoupled [see Fig. 1(a)] due to a different polarization, which is purely a compressional plasma displacement of the acoustic branch and incompressible plasma motion of the Alfvénic branch. In a torus Alfvénic and acoustic waves couple and their polarization is mixed. This type of coupling is mediated by the geodesic curvature and the plasma pressure, and is the focus of this paper.

As a result, various gaps in the continuum emerge [see Fig. 1(b)], such as the toroidicity-induced Alfvén eigenmode (TAE) gap due to poloidal m and $m+1$ Alfvénic harmonics coupling,[6] the BAE gap due to the GAM induced upshift of the Alfvénic continuum,[7] and the BAAE gap due to m Alfvénic and $m \pm 1$ acoustic branches coupling, which was studied in detail recently.[3,8] In each gap a corresponding global eigenmode can emerge. In addition, global modes are found near the extrema points of the continuum, such as those formed at the $q_{\min}$ location in the reversed shear plasma.

Because of the strong presence of the acoustic wave in the BAAE solution, as we will see, it is important to understand the role of the kinetic effects such as resonances with thermal ions. This will be the subject of this work.

The paper is organized as follows. In Sec. II we outline the ideal MHD and present kinetic theories. We compare the main BAAE properties with the experimental data from

[a)]Paper GI1 2, Bull. Am. Phys. Soc. **53**, 79 (2008).
[b)]Invited speaker. Electronic mail: ngorelen@pppl.gov.

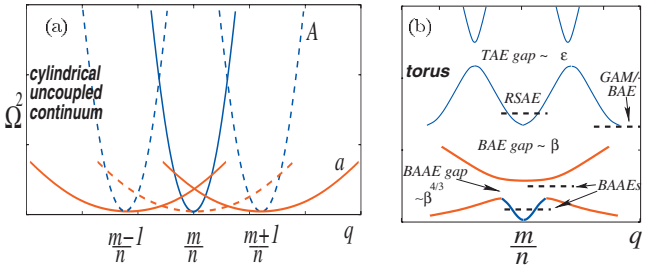

FIG. 1. (Color) Schematic of the low-frequency Alfvénic and acoustic continuum in a cylinder (a) and in a torus (b).

National Spherical Torus Experiment [NSTX (Ref. 9)] and DIII-D (Ref. 10) in Sec. III. In particular, the comparison of the ideal MHD and kinetic predictions for the instability frequency favors the kinetic theory. Effects on the confinement of energetic particles due to BAAEs are presented in Sec. IV. Results are discussed and summarized in Sec. V.

II. BAAE THEORY

Here we outline the ideal MHD theory,[3] which was recently developed to explain new observations of global eigenmodes in toroidal plasma experiments on NSTX and JET,[8] as well as on DIII-D experiments reported in this paper. BAAEs can appear in the frequency and location adjacent to the extremum points of the Alfvén-acoustic continuum. The extremum points exist in the zero shear region and inside the continuum gaps. It is the finite pressure, plasma compressibility, and the geodesic curvature that mediate Alfvén and acoustic branches coupling to form the gap structure,[4] called here the BAAE gaps.

The BAAE gap upper frequency, Ω_+, emerges when the $m\pm 1$ acoustic sideband frequencies match, $\Omega_{a,+}=\Omega_{a,-}$, and in ideal MHD, low beta and high-aspect-ratio plasmas are given by[3,4]

$$\Omega^2=\Omega_+^2=1/q^2, \tag{1}$$

where (and below) capitalized notations for frequencies denote normalization $\Omega^2\equiv\omega^2/\omega_s^2$, $\omega_s^2\equiv\delta(v_A/R_0)^2=v_s^2/R_0^2$, $\delta=\gamma\beta/2\ll 1$, $\Omega_{a\pm}=k_{\pm 1}$, $k_j=(m+j-nq)/q$ is parallel wavevector, n and m are the toroidal and poloidal wave numbers, and v_A and v_s are the Alfvén and acoustic (sound) speeds, respectively, and γ is the specific heat ratio. Near the rational magnetic surface, another branch, called here the modified Alfvén branch, "shielded" by acoustic sidebands exists,

$$\Omega^2=k_0^2/\delta(1+2q^2). \tag{2}$$

An important conclusion of the ideal theory is that the extremum point of the continuum, which exists at the $q_{\min}$ surface, follows the modified Alfvén branch dispersion, similar to the reversed shear Alfvén eigenmode (RSAE) case. Thus, if $q_{\min}$ decreases, the frequency sweeps up until it reaches the sideband acoustic branch, which gives an approximate value for the BAAE gap center, Ω_0. The lower gap frequency can be approximated as $\Omega_-=\Omega_+-2(\Omega_+-\Omega_0)$,

$$\Omega_-=[1-2\sqrt{\delta(1+2q^2)}]/q,$$

which agrees well with more accurate expression.[8] Global BAAE solutions corresponding to the continuum extremum points were found numerically. Away from the rational surface, at $k_0^2>\delta$ two acoustic $j=\pm 1$ sideband solutions exist.

A. BAAE kinetic theory

Because of the low frequency of BAAEs it is important to develop the kinetic theory of these modes, which should account for the resonance interaction with thermal ions. We make use of the dispersion relation applicable to the Alfvén-acoustic continuum.[11] It was derived from the quasineutrality condition and Ampere's law (similar kinetic dispersion relations were derived elsewhere[12,13]). One can straightforwardly generalize it to account for sideband parallel wavevector radial variation and electron drift effects as follows:

$$\frac{k_0^2+\Delta_{\rm MHD}^2}{\Omega_k^2\delta_k}=1-\frac{\Omega_{k*pi}}{\Omega_k}-\sum_{j=\pm 1}\frac{1}{2k_j^2}\left\{\frac{[\Omega_{k*pe}+\Omega_k\xi_{ji}N_j]N_j}{\Omega_k D_j\xi_{ji}^2}-\left(1-\frac{\Omega_{k*i}}{\Omega_k}\right)\frac{F_j}{\xi_{ji}}+\frac{\Omega_{k*Ti}}{\Omega_k}\frac{G_j}{\xi_{ji}}\right\}, \tag{3}$$

where coefficients N, D, F, and G are given in the Appendix, $\tau=z_i^2T_en_i/z_e^2T_in_e$, $\xi_{ji}=\omega/k_jv_{Ti}$, v_{Ti} is the thermal ion velocity, $\delta_k=\tau\beta_i/2$, $\Omega_k^2\equiv\Omega^2\delta/\delta_k$, subscript k is introduced to separate kinetic from ideal normalization, $\omega_{*j}=nqv_{Tj}^2/2\omega_{cj}rL_j$, L_j is the gradient scale length computed for the electron or ion densities, which are n_j, $j=e,i$, respectively, z_j is particle charge, $\Omega_{k*j}^2=\omega_{*j}^2\delta/\omega_s^2\delta_k$, $\Omega_{k*Tj}=\Omega_{k*j}\eta_j$, $\Omega_{k*pj}=\Omega_{k*j}(\eta_j+1)$, and $\eta_j=\partial\ln T_j/\partial\ln n_j$. Here we also introduced a shift to the mode eigenfrequency from the continuum, $\Delta_{\rm MHD}$, which has to be computed using global codes such as NOVA.[6] Although we show the way to include $\Delta_{\rm MHD}$ into the BAAE dispersion it will be neglected in the evaluations hereafter. The geodesic curvature coupling to the acoustic mode emerges from the curvature particle drift frequencies in the kinetic equation.[11,12,14] If contributions from two acoustic sidebands are considered to be the same, $k_{+1}^2\simeq k_{-1}^2$ or $k_0\ll 1/q$, and $\Omega_{k*pe}=0$, Eq. (3) is reduced to the dispersion obtained in Refs. 11 and 13. As we will show $j=\pm 1$ sideband contributions should be included separately to recover the MHD results outlined above. We note that electron drift frequencies in Eq. (3) appear from the quasineutrality condition and the vorticity equations of Ref. 15 [due to ω_{de} terms in Eqs. (39) and (41) of that reference] if trapped electrons are ignored. Earlier such ω_{de} and ω_{*pe} terms appeared in Ref. 16 and recently in Ref. 17. Similar dispersion, including ω_{*i} effects, was obtained from global gyrokinetic theory in Ref. 18.

Recently the existence of global electron drift-sound and drift-Alfvénic modes due to ω_{*e} was demonstrated in Ref. 19. Because of the two-fluid MHD model used in that work, ω_{*pe} effects and associated solutions were not found, neither were the potential ITG-like (ITG for ion temperature gradient) instabilities of the drift branches. These effects seem to be dominant in experimental conditions, where the temperature profile gradients are (typically) stronger than plasma density gradients.

Note also that in the derivation of the above equations it was assumed that the thermal ion parallel velocity is not changed during the characteristic time of the interaction with the mode. This is true if the bounce frequency of thermal ions is smaller than the mode frequency, that is $\sqrt{\beta_i \epsilon} < k_0$, which can be satisfied for sufficiently small ϵ and plasma pressure.

It is possible to show that when the ion temperature gradient is sufficiently large the BAAE instability can be driven purely by thermal ions. Next we consider two limit cases of the dispersion relation, Eq. (3).

1. Simple BAAE dispersion in electron dominated plasma, $\tau \gg 1$

Kinetic dispersion of the modified Alfvén branch in a plasma with dominant electron beta corresponds to the limit $\tau > 2\xi_i^2 \gg 1$. We analyze Eq. (3), first, in this limit, which becomes

$$\frac{k_0^2+\Delta_{\mathrm{MHD}}^2}{\Omega_k^2\delta_k} = 1 + 2q^2 \frac{\Omega_k - \Omega_{k*pi} - \Omega_{k*pe}}{\Omega_k - \Omega_{k*pi} - \xi_s^2(\Omega_k - \Omega_{k*e} + \tau\Omega_{k*i})} + \frac{\Omega_k - \Omega_{k*i}(1+\eta_i\xi_i^2)}{\Omega_k - \Omega_{k*pi}} \times \left(1 - \frac{2\Omega_{k*pe}}{\Omega_k - \Omega_{k*pi}}\right) \xi_s^3 \tau^{3/2} e^{-\xi_s^2\tau/2} \frac{i\sqrt{\pi}\sigma q^2}{2\sqrt{2}}, \tag{4}$$

where $\sigma = 0, 1, 2$ for $\Im\Omega_k < 0, =, > 0$, respectively, $\xi_{\pm 1i} \simeq \omega q R / v_{Ti} = \omega q \sqrt{\tau}/\omega_A \sqrt{\beta_e} \equiv \xi_s \sqrt{\tau/2}$, and for BAAEs $\xi_s < 1$. Also $\xi_s = \Omega_k / \Omega_{k+}$.

If drift frequencies are ignored we find

$$\frac{k_0^2+\Delta_{\mathrm{MHD}}^2}{\Omega_k^2\delta_k} \simeq 1 + \frac{2q^2}{1-\xi_s^2}\left(1 + \xi_s^3\tau^{3/2}e^{-\xi_s^2\tau/2}\frac{i\sqrt{\pi}\sigma}{2\sqrt{2}}\right). \tag{5}$$

If its imaginary part is neglected and $\xi_s \ll 1$, Eq. (5) is reduced to the MHD dispersion, Eq. (2), and corresponds to the sweeping up BAAE solution. Its real part can be written in the form

$$\Omega_{k0}^2 = \frac{k_0^2+\Delta_{\mathrm{MHD}}^2}{\delta_k\{1 + 2q^2/[1 - k_0^2 q^2/\delta_k(1+2q^2)]\}}. \tag{6}$$

The damping of this solution is exponentially small. Defining the imaginary part of the normalized frequency as $\gamma \equiv \Im\Omega_k$ we find

$$\frac{\gamma}{\Omega_{k0}} = -\xi_s^3\tau^{3/2}e^{-\xi_s^2\tau/2}\frac{q^2}{1+2q^2}\frac{\sqrt{\pi}\sigma}{2\sqrt{2}}. \tag{7}$$

2. Low ξ_i BAAE dispersion

Here we consider another limit case, $\xi_{\pm 1i} \ll 1$, which allows for finite τ. We find then from Eq. (3)

$$\frac{(k_0^2+\Delta_{\mathrm{MHD}}^2)\Omega_k}{\Omega_k^2\delta_k} \simeq \frac{H}{\Omega_k - \Omega_{k*e}/(1+\tau)} + \left[\Omega_k - \Omega_{k*i} - \frac{3\Omega_{k*Ti}}{2} - \tau\Omega_{k*pe}\frac{\Omega_k - \Omega_{k*i} - \Omega_{k*Ti}/2}{\Omega_k(1+\tau) - \Omega_{k*e}}\right]\frac{iq^2\sqrt{\pi}e^{-\xi_s^2\tau/2}}{\xi_s\sqrt{2\tau}}, \tag{8}$$

where

$$\frac{H}{\Omega_k - \Omega_{k*e}/(1+\tau)} = (\Omega_k - \Omega_{k*pi})\left(1 + \frac{q^2}{2}\right) + \frac{\pi\tau q^2}{4}\frac{(\Omega_k - \Omega_{k*i} - \Omega_{k*Ti}/2)^2}{\Omega_k(1+\tau) - \Omega_{k*e}} - \frac{\pi q^2\tau^2}{2}\Omega_{k*pe}\frac{(\Omega_k - \Omega_{k*i} - \Omega_{k*Ti}/2)(\Omega_k - \Omega_{k*i} + \Omega_{k*Ti}/2)}{(\Omega_k(1+\tau) - \Omega_{k*e})^2}.$$

Strong ion Landau damping occurs due to the acoustic sidebands resonance with thermal ions. We note that this equation gives good approximation even for finite $\xi_i < 1$.

a. Drift frequency solution In the presence of drift diamagnetic frequencies Eq. (8) has solutions with positive $\Omega_k \sim \Omega_{k*Ti}$ and negative $\Omega_k \sim \Omega_{k*Te}$ frequencies. At $k_0 \simeq 0$ one can find asymptotic solutions of this equation if drift frequencies are small in comparison with BAAE gap frequency $|\Omega_k| \sim |\Omega_{k*Ti,e}| \ll \Omega_{k+}$. Solutions emerge from the condition that the in the square brackets of the second term of the right-hand side (RHS) of Eq. (8) is zero,

$$\Omega_k = \Omega_{k1,2} = \frac{\Omega_{k*i}}{2}\left\{1 + \frac{3\eta_i}{2} + \frac{\Omega_{k*e}}{\Omega_{k*i}}\left(1 + \frac{\tau\eta_e}{(1+\tau)}\right) \pm \sqrt{\left[1 + \frac{3\eta_i}{2} + \frac{\Omega_{k*e}}{\Omega_{k*i}}\left(1 + \frac{\tau\eta_e}{(1+\tau)}\right)\right]^2 - \frac{4\Omega_{k*e}\left[1 + \frac{3\eta_i}{2} + \tau(1+\eta_e)\left(1 + \frac{\eta_i}{2}\right)\right]}{\Omega_{k*i}(1+\tau)}}\right\} \tag{9}$$

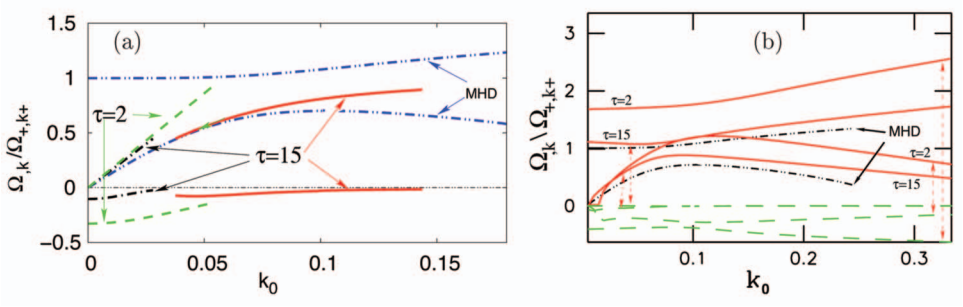

FIG. 2. (Color) BAAE continuum solutions comparison with the MHD solution as indicated. All real parts of the solution frequencies are positive and their imaginary parts are negative. Frequencies are normalized to $\Omega_{k+}=1/q$ for kinetic solutions or $\Omega_+=1/q$ for MHD solutions. In (a) two kinetic branches are shown for $\tau=15$, lower frequency, Eq. (8) [with the real frequency from Eq. (10)], and higher frequency, Eqs. (6) and (7) solutions. Equation (8) dispersion is also shown for $\tau=2$. (b) presents frequencies evaluated using general dispersion relation, Eq. (3). Results are shown for $n=12$, $m=21$, and $\delta=\delta_k=0.25\%$.

which can is directly verifiable by solving Eq. (3) numerically. Here subscript indices 1 and 2 correspond to plus and minus signs in the RHS of Eq. (9). Solution Ω_{k1} is an ion branch with a positive frequency and Ω_{k2} is an electron branch with a negative frequency. An ion solution can be identified as a kinetic ballooning mode (KBM). The ion branch Ω_{k1} is reduced to an earlier obtained solution in Ref. 13 if $\Omega_{k*e} \ll \Omega_{k*i}$,

$$\Omega_{k1} = \Omega_{k*i}\left(1 + \frac{3\eta_i}{2}\right).$$

Corresponding growth rates of these two branches are found by a perturbation method assuming that $\gamma_{1,2} \ll \Omega_{k1,2}$,

$$\gamma_{1,2} = \frac{\Omega_{k1,2}\sqrt{2\tau}(-1)^{1,2}}{\Omega_{k+}q^2\sqrt{\pi}e^{-\xi_s^2\tau/2}(\Omega_{k2}-\Omega_{k1})} H|_{\Omega_{k1,2}}.$$

The instability is expected for both electron and ion branches provided $\eta_{e,i}$ are sufficiently large.

b. Sweeping up BAAE solution At frequencies above the drift frequencies the approximate solution for the *unstable* mode is obtained,

$$\Omega_k^2 = \frac{k_0^2 + \Delta_{\mathrm{MHD}}^2}{\delta_k\left[1 + q^2\left(\frac{1}{2} + \frac{\pi}{4}\frac{\tau}{1+\tau}\right)\right]}. \tag{10}$$

As we will show later, this expression provides dependence close to the numerical one even though we ignored its imaginary part.

3. Comparisons with numerical solutions of Eq. (3)

Equation (3) also contains acoustic branches which correspond to the zero denominator of the second term in the curl brackets of its left hand side. This branch is the same as in MHD, Eq. (1), for $\tau \gg 1$, but needs to be analyzed numerically otherwise. Figure 2 shows the comparison of these limiting cases at $\Omega_{k*T,i,e}=0$ with MHD and with the general dispersion. The numerical evaluation of Eq. (3) shows that the damping rate of its branches increases rapidly when $\tau<2$. Quantitatively, in such a case the damping rate at the extremum points inside the BAAE continuum gap is large $|\gamma/\Omega_k| > \sim 25\%$. The modified Alfvén branch damping becomes comparable (or larger) to the frequency at smaller frequencies.

We examine the drift frequency effects by analyzing the general dispersion relation Eq. (3) with the plasma parameters close to ones from DIII-D experiments. In NSTX, with low n numbers observed, drift frequencies can be neglected. We fix $\tau=2$, $\delta_k=0.6\%$, drift frequencies $\Omega_{k*i}=\Omega_{k*e}=0$, $\Omega_{k*Ti}=0.94\Omega_{k+}$ for $n=8$, $\Omega_{k*Te}=-3\Omega_{k*Ti}/2$, and $q_{\min}=2$ when $k_0=0$. As shown in Fig. 3 in simulations we have found both ion and electron branches to be unstable at $k_0=0$ with the frequencies determined by the drift frequencies, $\sim 2\Omega_{k*Ti}/3$ and $\sim -\Omega_{k*Ti}/3$. Note that in the considered example our analytical result, Eq. (9), gives $\Omega_{k1}=\Omega_{k*Ti}$ and $\Omega_{k2}=-\Omega_{k*Ti}/2$, which are only approximately close to the results shown in Fig. 3 at $k_0=0$. This is because of the chosen relatively high drift frequency. The ion branch solution trans-

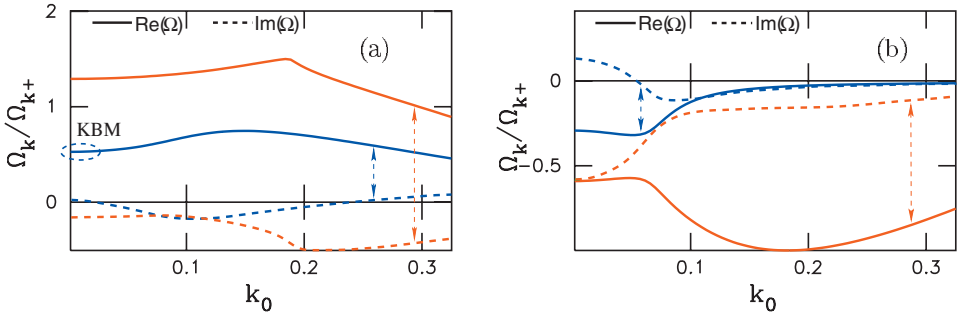

FIG. 3. (Color) Alfvén-acoustic continuum with finite drift frequencies. (a) shows two ion branches and (b) shows two electron branches. Only the least stable solutions are plotted.

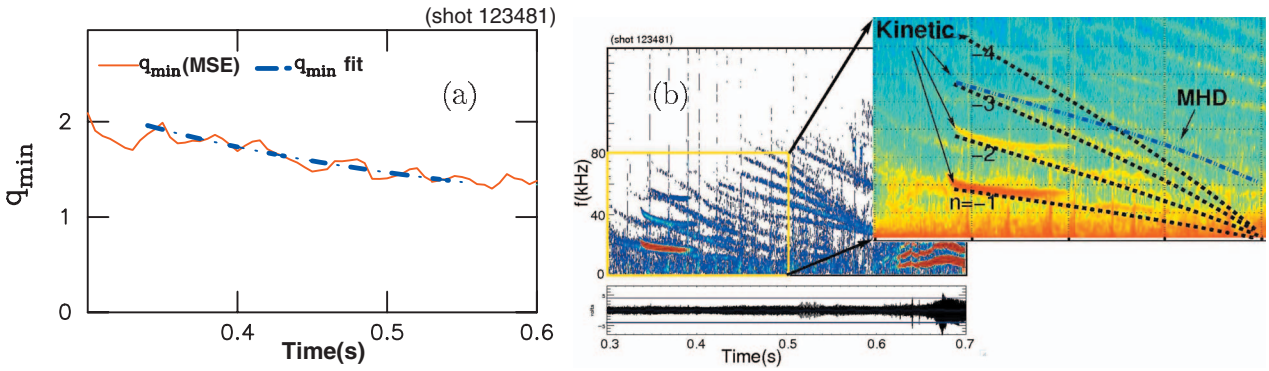

FIG. 4. (Color) MSE measured evolution of the minimum value of the safety factor, $q_{\min}$, and its fit (a). Shown in figure (b) is the NSTX magnetic signal spectrum for the shot No. 123481, measured at the plasma edge. In the inset of (b) the frequency spectrum is zoomed and overlaid with the kinetic (for $n=-1$ to -4) and MHD (shown for $n=-3$ only) dispersion frequencies.

forms to the BAAE gap branch away from the rational surface $k_0 > \sqrt{2\delta_k}$. One can also see that the damping rate of the obtained BAAE solutions in this case, $\tau=2$, is much smaller $\gamma/\Omega_k \sim -10\%$ than without drift frequency effects from $\sim -25\%$ [compare to Fig. 2(b)]. This is because of the destabilization due to Ω_{k*Ti} terms in the third term of the RHS of Eq. (8).

We note that the drift frequency mode drive is due to ITG, which is the same drive as in the earlier higher frequency Afvénic ITG mode studies.[20] One important conclusion we draw from the kinetic versus MHD theory comparison is that the kinetics improves and complements the MHD framework for BAAE studies. It properly addresses coupling to the acoustic wave and introduced ion Landau damping. However, qualitatively the kinetic theory agrees with the ideal MHD in a way that the acoustic and Alfvén branches are coupled and form the gap in the continuum. Thus the ideal MHD tools such as numerical codes can be applied for the BAAE analysis provided that the frequencies are normalized to the values, which follow from the kinetic theory. In this sense it is sufficient to develop a local kinetic theory using the ballooning formalism, i.e., assuming $k_r \gg k_\theta$.

III. COMPARISON WITH EXPERIMENTS

In JET experiments BAAE magnetic activity was observed with the characteristic frequency sweep up.[3] However, the frequency of $n=4$ gap BAAE was found to be ~ 1.8 times higher than measured. In those experiments the safety factor profile was not measured during BAAE activity and it was assumed that the q-profile is monotonic and $\tau=1$. A plausible and rather simple way to resolve this frequency mismatch was suggested in Ref. 8. It was proposed that local low (or slightly reversed) shear region exists with $q \simeq q_{\min} = 3/2$. Another assumption was that the plasma was dominated by electrons ($T_e \gg T_i$). In that case we evaluate $f_+ \simeq 21$ kHz, so that the inferred gap BAAE frequency ~ 16 kHz becomes sufficiently close to the Doppler shifted observed frequency $f=14$ kHz. This conjecture was supported by the presence of only even toroidal mode numbers in the magnetic signal spectrum, which follows from the requirements that $m=q_{\min} n$ must be integer. Similar sweeping modes in NSTX also showed even numbers at measured $q_{\min}=3/2$.[8] Kinetic expressions in JET plasma conditions are expected to agree with ideal MHD because $\delta_k=\beta_e/2=\delta$ since $\beta \simeq \beta_e$ and $\gamma \simeq 1$ for strongly ion cyclotron resonance frequency (ICRF) heated plasma, when most of the energy of H-minority is transferred to electrons.

BAAEs in NSTX were identified based on their frequency sweeping behavior, mode structure and its dynamics.[8] Qualitatively similar to theoretical predictions the BAAE frequencies swept up in experiments from a level close to the plasma rotation ($f_{\rm rot} \simeq 15$ kHz) at the $q_{\min}$ (sweep starts at $q_{\min}=3/2$) surface to about 50 kHz (for $n=2$ mode) in the laboratory frame. Detailed measurements of BAAE internal structure revealed the same radial localization, eigenfrequency (within measured accuracy), and their evolution as calculated by ideal MHD code NOVA. BAAEs in NSTX typically stay near the modified Alfvén continuum frequency and do not enter the Alfvén-acoustic gap, which is at ~ 25 kHz in the plasma frame. In NSTX plasmas typically $\tau \sim 1$ so that BAAE instability is possible only if the drive is strong, which can be expected because the fast ion pressure is comparable with the pressure of thermal ions.

A. Kinetic versus ideal MHD dispersion and NSTX data

Here we show new observations from NSTX where multiple instabilities were excited. The time scale of these instabilities is relatively long so that the measured $q_{\min}$ evolution allows for more accurate comparison of both the ideal MHD and kinetic dispersions with the experiments. In Fig. 4(a) $q_{\min}$ versus time is shown along with its fitted time dependence used in evaluating the mode frequency. In Fig. 4(b) we plot the kinetic and ideal MHD (as indicated) predictions for BAAE frequencies taking into account the plasma rotation $f=f_{\rm BAAE}+nf_{\rm rot}$, $f_{\rm rot}(q_{\min})=19-23$ kHz, n between -1 and -4. Because of the negative toroidal mode numbers and $f_{\rm BAAE}$ being close to zero, the instabilities are observed with frequency down sweeps instead of up sweeps, which is similar to the RSAE case reported earlier.[21] In NSTX drift frequencies can be neglected $f_{*pi}|_{n=1} \simeq 2$ kHz $\ll f_{\rm BAAE}$.

Plotted kinetic frequencies correspond to the real part of the modified Alfvénic solution at $T_i=T_e$, $\Re\omega_{\rm BAAE} \simeq v_A k_\parallel / \sqrt{1+q_{\min}^2(1/2+\pi/8)}$ [see Eq. (10)], whereas MHD

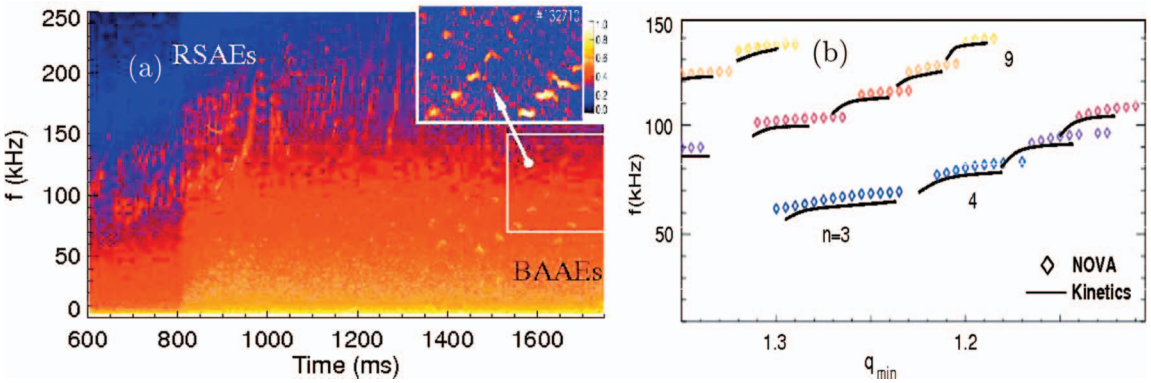

FIG. 5. (Color) The combined power spectrum of ECE and CO_2 interferometer (a) for DIII-D shot No.132710 taken at $R=1.93m$ and a zoom of a narrow region of several BES channels cross correlation are shown in the inset. (b) shows the results of NOVA simulations (points) of different n modes as indicated. Under each mode point shown as the black line is the lower continuum gap frequency from kinetic dispersion.

frequency is $v_A k_\parallel/\sqrt{1+2q_{\min}^2}$ [see Eq. (2)]. One can observe that the MHD dispersion notably deviates from the measured signal (yellow signal traces in the insert). Although the kinetic theory BAAE frequency is surprisingly close to the observations as can be seen from the insert on Fig. 4(b), we have to note that the plotted kinetic solution corresponds to the stable mode dispersion. Moreover because of strong damping of this solution the required equally strong drive can also change the real part of the frequency. This remains an issue for further studies, but the observed agreement with the stable kinetic mode frequency should be a constraint in developing the theory of BAAE instability.

B. Measurements of BAAEs in DIII-D

In dedicated experiments on DIII-D low-frequency instabilities, which can be identified as BAAE oscillations were also observed. Detailed measurements of internal low-frequency oscillations shown in Fig. 5(a) with the beam emission spectroscopy (BES), CO_2 interferometer, and electron cyclotron emission (ECE) diagnostics reveal very low-frequency signal peaks below the characteristic RSAE frequency signal. Experiments were conducted with the ECH applied at 0.8 s after which strong broadband oscillations are seen in Fig. 5(a). At a later time T_e increases, $\tau\sim 2$, and narrow BAAE peaks are seen in both BES and ECE spectra. Part of the reason for this is the signal enhancement due to the elevated electron temperature gradient. These modes have localized radial structure near $q_{\min}$. At $t=1.6$ s the plasma is characterized by $R_0=1.66$ m, $a=0.64$ m, $\beta_{pl0}=5\%$, $B_0=2$ T, $q_1\simeq 6$, and $q_{\min}\simeq 1.25$.

In order to identify observed instabilities we have performed a search for eigenmodes using the NOVA code and have found gap solutions with the frequencies shown in Fig. 5(b). Plotted values include the Doppler correction due to the plasma rotation 11.5 kHz at $q_{\min}$. NOVA finds solutions only as gap modes. During the sweeping up phase (modified Alfvén branch) all numerical solutions strongly interacted with the continuum and are discarded. Kinetic branch dispersion relation frequencies are also plotted, except for those values for which thermal ion Landau damping, Eq. (8), satisfies $|\gamma/\Omega_k|<0.25$ and $0<k_0<0.25$. Kinetic frequencies are plotted as sweeping up solutions transitioning to the gap frequency. The upper limit of k_0 is chosen to make the duration similar to NOVA simulations. The latter results from the global mode existence condition, which means weak interaction with the continuum.

Global NOVA BAAE solution eigenfrequencies adjusted to match the ideal and kinetic continua are close to the kinetic continuum gap frequency. They also show similar time duration to those observed [see insert on Fig. 5(a)]. The n sequence of instabilities is also reproduced. However, in the experiments there was no discernible BAAE activity on edge magnetics so a toroidal mode number determination was not possible. In the modeling the BAAE gap frequency is on the order 30–40 kHz in the plasma frame for that time.

The ECE diagnostic was used to measure the radial structure of BAAEs, an example of which is shown in Figs. 6(a) and 6(b), corresponding to the peak on the ECE spectrum diagram at $t=1590$ ms and $f=87$ kHz, as shown in Fig. 5(a). The mode structure is narrow in radial direction and localized near the $q_{\min}$ surface. One can relate the electron temperature to the plasma perturbation via the equation

$$\delta T_e = -\vec{\xi}\nabla T_e - (\gamma_e - 1)\mathrm{div}\,\vec{\xi},$$

where $\vec{\xi}$ is the plasma displacement and γ_e is the specific heat ratio computed for electrons. Since for low-frequencies oscillations, δT_e is expected to be constant along the magnetic field lines we can allow $\gamma_e=1$. Thus the contribution from the compressibility vanishes and δT_e amplitude is expected to be comparable on the low field side (LFS) and high field side (HFS) of the plasma midplane. This is consistent with the data shown in Fig. 6(a). With the amplitude of δT_e from Fig. 6(a) we evaluate the radial component of the plasma displacement: $\xi_r/a\simeq 3\times 10^{-3}$. This is comparable to the typical displacement reported for RSAE/TAE instabilities in similar DIII-D discharges.[22]

The NOVA computed BAAE radial displacement structure for $n=5$ is shown in Fig. 6(c) and is comparable with the experiment with regard to the mode location and the radial width. Further comparison using the synthetic diagnostic in

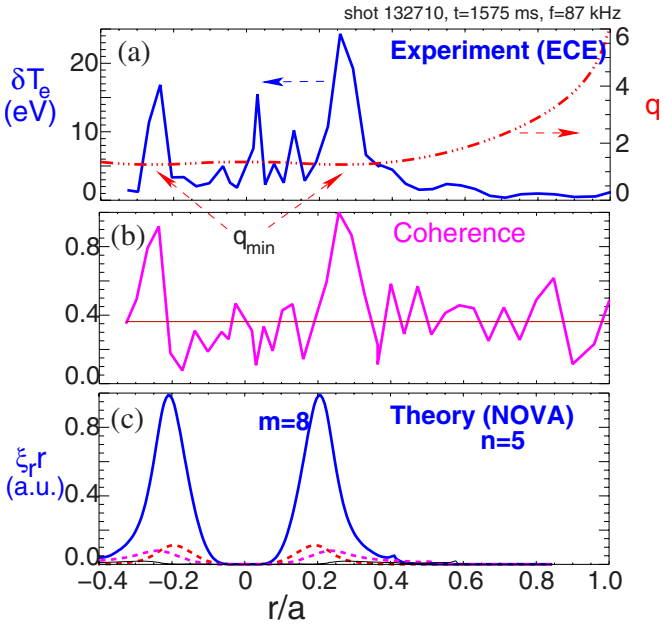

FIG. 6. (Color online) The ECE measured BAAE radial structure (a) and the signal phase coherence (b) for each radial channel point vs. minor radius. For comparison we also show the radial displacement of the simulated $n=5$ BAAE structure in figure (c) using ideal code NOVA. Dominant harmonic $m=8$ is indicated and the sideband harmonics are plotted as a dashed lines. The safety factor profile is shown in figure (a).

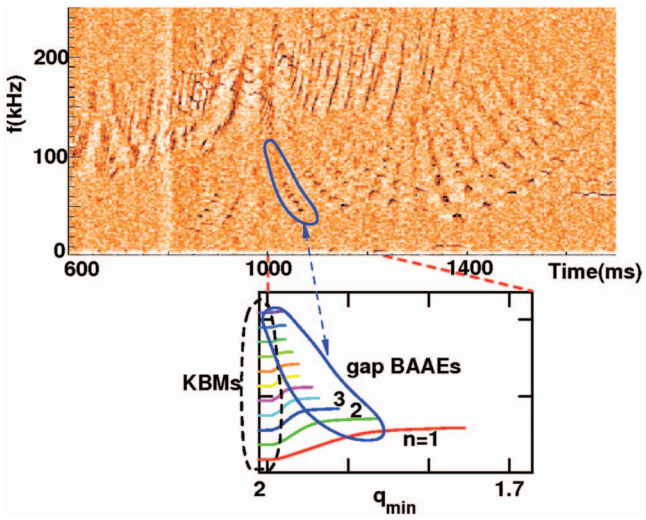

FIG. 7. (Color) DIII-D shot No. 132238 instability frequency spectrum (a) [the same as in Fig. 5(a) but with a different color map] and the kinetic theory predictions for the transition from KBM to BAAE branches (b), shown for n-numbers from 1 to 11.

NOVA can produce a better agreement.[23] The small shift toward the center can be due to the specific gap structure and is sensitive to the mode number.

C. Drift effects and BAAEs in DIII-D

Because in DIII-D the drift frequency is significant, the question which needs to be addressed is whether the observed modes are related to the electron drift mode, KBM or BAAE branches. We rely on the measurements such as the BES diagnostic, which indicates that the mode is propagating in the ion direction. Without addressing the stability issue we plot the predictions of the kinetic dispersion for another DIII-D shot No. 132238 in Fig. 7 (insert) for different values of $n=1-11$. In that figure we see again the transition from the KBM branch at $q_{\min}=2$ to BAAE as the safety factor decreases. If KBMs are excited the observed peaks would be seen simultaneously in time, i.e., aligned at one time on the spectrogram. Opposite to this, BAAE gap mode instabilities are expected to form patterns similar to ones observed [one of them is encircled on that Fig. 7(a)]. Note that global KBMs also can be excited by fast ions if the drive is sufficiently strong, as was suggested earlier.[24]

D. Evaluating BAAE frequency in DIII-D

Because of the uncertainty in the q profile on JET and in NSTX absolute value of BAAE frequency was not satisfactorily compared with the theoretical predictions. It turns out that DIII-D data can be used for such frequency comparison despite the unavailability of n measurements. By plotting the proper local dispersion frequency patterns near $t=1300$ ms for the shot No. 132238 one can show that the signal peak at $t=1375$ ms and $f=41$ kHz corresponds to $n=2$, Fig. 7. With the local rotation frequency $f=9.5$ kHz we find that the mode has $f=22$ kHz in the plasma frame. Electron and ion temperatures in that shot were $T_i=1.9$ keV and $T_e=2.46$ keV, respectively, so that $\tau \sim T_e/T_i=1.3$. Kinetic dispersion relation finds $\Re\Omega_{k-}=1.1$ and $\Re\Omega_{k+}=1.7$ for this case. Evaluating Ω_{k+} normalization frequency one can find that it corresponds to 17.6 kHz. This implies for the lower and upper BAAE gap limits, 19 and 30 kHz, respectively, which sets the measured $n=2$ BAAE frequency, 22 kHz near the bottom of the gap. This is where NOVA finds the global gap BAAE frequency as shown in Fig. 5(b) (for higher n-values).

IV. EFFECTS ON ENERGETIC PARTICLES

BAAEs in NSTX can form avalanches in which case several modes are excited simultaneously and result in strong beam ion redistribution and loss. In one example this was evidenced by a 13% neutron signal drop, which approximately indicates the same amount of beam ion loss.[25] Energetic particle radial transport can be further enhanced by nonlinear coupling to TAEs.[26]

In DIII-D the fast ion D-alpha (FIDA) diagnostic,[27] capable of measuring the beam ion profiles, suggests that BAAEs increase fast ion transport to a level comparable to that due to RSAEs reported in DIII-D.[22] Figure 8 represents such measurements at a time when the ECE spectrum activity is dominated by BAAEs as can be seen from Fig. 5(a). Measured beam ion profiles are compared to the classical predictions on the basis of computing fast ion distribution function when all the collective instabilities are neglected. One can see from the comparison that the beam ion profiles are depleted from $r/a=0$ up to $r/a \simeq 0.7$, whereas the modes are relatively narrow in radial direction, Fig. 6(c). These results show that the core beam ion density is reduced approximately by half.

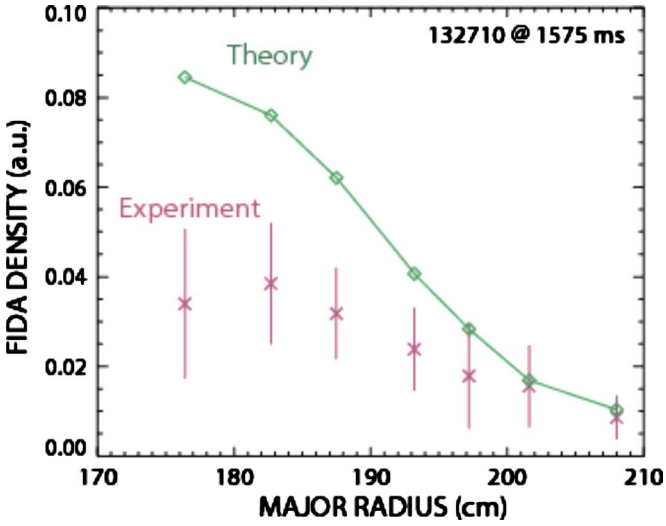

FIG. 8. (Color online) Measured FIDA energetic particle density profile (experiment) compared to the FIDA density profile calculated using the classical fast ion distribution function from TRANSP (theory). The "FIDA density" is the radiance over blueshifted wavelengths that correspond to energies of $E_\lambda = 30-60$ keV, divided by the local density of injected neutrals for DIII-D shot No. 132710 at $t = 1571$ ms.

We note that earlier numerical simulations were not able to reproduce the same level of fast ion transport as in the experiments based on only RSAE and TAE modes.[22] Our results indicate that BAAEs should also be included in such simulations.

V. DISCUSSION AND SUMMARY

Our theoretical and experimental studies further confirm the previous results of BAAE investigations on JET and NSTX.[3,8] Key elements of the mode identification and the theory experiment comparison are the instability frequency spectrum and the trends in observable instability properties as plasma parameters evolved.

In global simulations these eigenmodes exist in the Alfvén-acoustic continuum gaps and in the regions of low shear adjacent to the continuum extremum points. One of our results is that Alfvén-acoustic gap exists in both ideal MHD and in the kinetic theory. If the electron temperature exceeds the thermal ion temperature, the kinetic BAAE dispersion is close to that from MHD and the modes have weak damping. In the opposite case, when electron and ion temperatures are comparable, the ion Landau damping is strong, but is reduced if thermal ion drift frequency is significant like in the DIII-D case. Observed BAAE frequencies within the experimental uncertainty agree with the kinetic theory. Ideal MHD theory produces a similar BAAE gap, which should be properly normalized to the kinetic theory frequencies so that MHD codes can be used to simulate the global gap BAAE mode structure. The sweeping mode structure can be modeled if the drift frequency is small like in the case of NSTX or in DIII-D with low-n numbers. Drift effects do modify the BAAE dispersion. KBMs and electron drift branches are recovered in the kinetic theory but do not seem to be observed in the experiments. The main effect of drift frequencies on BAAE excitation in experiments is predicted to be destabilizing due to ITG drive.

We have shown that BAAE mode structure and localization measured in DIII-D [and earlier in NSTX (Ref. 8)] agree with theoretical predictions. We also presented results of BAAE induced beam ion radial transport in DIII-D implied by the FIDA diagnostic measurements. FIDA data shows up to 50% depletion of confined beam ions near the plasma center when the instability spectrum is dominated by BAAEs. Since these instabilities can strongly interact with the thermal ions and be destabilized by ITG one can elucidate such an effect as α-channeling,[28] when energy is directly deposited into the background ions while avoiding heating electrons. Future work should address the investigation of the instability polarization and numerical studies making use of global codes properly accounting for the kinetics effects and drive from fast ions.

ACKNOWLEDGMENTS

This work supported in part by the U.S. Department of Energy under Contract No. DE-AC02-76CH03073.

APPENDIX: KINETIC INTEGRALS FOR IONS AND ELECTRONS

Here we list expressions for the kinetic coefficients in Eq. (3), which are a direct generalization of the corresponding coefficients of Ref. 11,

$$N_j = \left(1 - \frac{\Omega_{k*i}}{\Omega_k}\right)\left[\xi_{ji} + \left(\xi_{ji}^2 + \frac{1}{2}\right)Z_j\right] - \frac{\Omega_{k*Ti}}{\Omega_k}\left[\xi_{ji}\left(\xi_{ji}^2 + \frac{1}{2}\right) + \left(\xi_{ji}^4 + \frac{1}{4}\right)Z_j\right], \tag{A1}$$

$$D_j\xi_{ji} = \frac{1}{\tau}\left(1 - \frac{\Omega_{k*e}}{\Omega_k}\right) + 1 + \left(1 - \frac{\Omega_{k*i}}{\Omega_k}\right)\xi_{ji}Z_j - \frac{\Omega_{k*Ti}}{\Omega_k}\xi_{ji}\left[\xi_{ji} + \left(\xi_{ji}^2 - \frac{1}{2}\right)Z_j\right], \tag{A2}$$

$$F_j = \left(\xi_{ji}^2 + \tfrac{3}{2}\right)\xi_{ji} + \left(\xi_{ji}^4 + \xi_{ji}^2 + \tfrac{1}{2}\right)Z_j, \tag{A3}$$

$$G_j = \xi_{ji}[\xi_{ji}^4 + \xi_{ji}^2 + 2] + \left(\xi_{ji}^6 + \frac{\xi_{ji}^4}{2} + \xi_{ji}^2 + \frac{3}{4}\right)Z_j, \tag{A4}$$

where $Z_j = Z(\xi_{ji}) \equiv \pi^{-1/2}\int e^{-t}dt/(t-\xi_{ji})$ is the plasma dispersion function.

[1] P. H. Diamond, S.-I. Itoh, K. Itoh, and T. S. Hahm, Plasma Phys. Controlled Fusion **47**, R35 (2005).
[2] W. W. Heidbrink, E. J. Strait, M. S. Chu, and A. D. Turnbull, Phys. Rev. Lett. **71**, 855 (1993).
[3] N. N. Gorelenkov, H. L. Berk, E. Fredrickson, and S. E. Sharapov, Phys. Lett. A **370**, 70 (2007).
[4] B. van der Holst, A. J. C. Beliën, and J. P. Goedbloed, Phys. Plasmas **7**, 4208 (2000).
[5] G. T. A. Huysmans, W. Kerner, D. Borba, H. A. Holties, and J. P. Goedbloed, Phys. Plasmas **2**, 1605 (1995).
[6] C. Z. Cheng and M. S. Chance, Phys. Fluids **29**, 3695 (1986).

[7]M. S. Chu, J. M. Greene, L. L. Lao, A. D. Turnbull, and M. S. Chance, Phys. Fluids B **4**, 3713 (1992).
[8]N. N. Gorelenkov, H. L. Berk, N. A. Crocker, E. D. Fredrickson, S. Kaye, S. Kubota, H. Park, W. Peebles, S. A. Sabbagh, S. E. Sharapov, D. Stutmat, K. Tritz, F. M. Levinton, and H. Yuh, Plasma Phys. Controlled Fusion **49**, B371 (2007).
[9]S. M. Kaye, M. G. Bell, R. E. Bell, J. Bialek, T. Bigelow, M. Bitter, P. Bonoli, D. Darrow, P. Efthimion, J. Ferron, E. Fredrickson, D. Gates, L. Grisham, J. Hosea, D. Johnson, R. Kaita, S. Kubota, H. Kugel, B. LeBlanc, R. Maingi, J. Manickam, T. K. Mau, R. J. Maqueda, E. Mazzucato, J. Menard, D. Mueller, B. Nelson, N. Nishino, M. Ono, F. Paoletti, S. Paul, Y-K. M. Peng, C. K. Phillips, R. Raman, P. Ryan, S. A. Sabbagh, M. Schaffer, C. H. Skinner, D. Stutman, D. Swain, E. Synakowski, Y. Takase, J. Wilgen, J. R. Wilson, W. Zhu, S. Zweben, A. Bers, M. Carter, B. Deng, C. Domier, E. Doyle, M. Finkenthal, K. Hill, T. Jarboe, S. Jardin, H. Ji, L. Lao, K. C. Lee, N. Luhmann, R. Majeski, S. Medley, H. Park, T. Peebles, R. I. Pinsker, G. Porter, A. Ram, M. Rensink, T. Rognlien, D. Stotler, B. Stratton, G. Taylor, W. Wampler, G. A. Wurden, X. Q. Xu, and L. Zeng, Phys. Plasmas **8**, 1977 (2001).
[10]J. L. Luxon, Nucl. Fusion **42**, 614 (2002).
[11]F. Zonca, L. Chen, and R. Santoro, Plasma Phys. Controlled Fusion **38**, 2011 (1996).
[12]A. B. Mikhailovskii, Nucl. Fusion **13**, 259 (1973).
[13]A. B. Mikhailovskii and S. E. Sharapov, Plasma Phys. Rep. **25**, 838 (1999).
[14]A. B. Mikhailovskii, Zh. Eksp. Teor. Fiz. **68**, 1772 (1975) [Sov. Phys. JETP **41**, 890 (1975)].
[15]C. Z. Cheng and N. N. Gorelenkov, Phys. Plasmas **11**, 4784 (2004).
[16]A. Hirose, L. Zhang, and M. Elia, Phys. Rev. Lett. **72**, 3993 (1994).
[17]A. I. Smolyakov, C. Nguyen, and X. Garbet, Plasma Phys. Controlled Fusion **50**, 115008 (2008).
[18]P. Lauber, S. Günter, M. Brüdgam, M. G. Munoz, S. da Graca, N. Hicks, V. Igochine, and M. Maraschek, *35th European Physical Society Conference on Plasma Physics* (European Physical Society, Hersonissos, Greece, 2008), Paper No. O4.030.
[19]Y. Kolesnichenko, V. Lutsenko, A. Weller, H. Thomsen, Y. Yakovenko, J. Geiger, and A. Werner, in Proceedings of the 22nd IAEA Fusion Energy Conference, Geneva, Switzerland, 2008.
[20]F. Zonca, L. Chen, J. Q. Dong, and R. A. Santoro, Phys. Plasmas **6**, 1917 (1999).
[21]R. Nazikian, H. L. Berk, R. V. Budny, K. H. Burrell, E. J. Doyle, R. J. Fonck, N. N. Gorelenkov, C. Holcomb, G. J. Kramer, R. J. Jayakumar, R. J. La Haye, G. R. McKee, M. A. Makowski, W. A. Peebles, T. L. Rhodes, W. M. Solomon, E. J. Srait, M. A. Van Zeeland, and L. Zeng, Phys. Rev. Lett. **96**, 105006 (2006).
[22]W. W. Heidbrink, N. N. Gorelenkov, Y. Luo, M. A. Van Zeeland, R. B. White, M. E. Austin, K. H. Burrell, G. J. Kramer, M. A. Makowski, G. R. McKee, and R. Nazikian, Phys. Rev. Lett. **99**, 245002 (2007).
[23]M. A. Van Zeeland, M. E. Austin, N. N. Gorelenkov, W. W. Heidbrink, G. J. Kramer, M. A. Makowski, G. R. McKee, R. Nazikian, E. Ruskov, and A. D. Turnbull, Phys. Plasmas **14**, 056102 (2007).
[24]N. N. Gorelenkov and W. W. Heidbrink, Nucl. Fusion **42**, 150 (2002).
[25]D. Darrow, E. Fredrickson, N. Gorelenkov, A. Roquemore, and K. Shinohara, Nucl. Fusion **48**, 084004 (2008).
[26]E. D. Fredrickson, R. E. Bell, D. Darrow, G. Fu, N. N. Gorelenkov, B. P. LeBlanc, S. S. Medley, J. E. Menard, H. Park, A. L. Roquemore, W. W. Heidbrink, S. A. Sabbagh, D. Stutman, K. Tritz, N. A. Crocker, S. Kubota, W. Peebles, K. C. Lee, and F. M. Levinton, Phys. Plasmas **13**, 056109 (2006).
[27]Y. Luo, W. Heidbrink, K. Burrell, D. Kaplan, and P. Gohil, Rev. Sci. Instrum. **78**, 033505 (2007).
[28]N. J. Fisch and J.-M. Rax, Phys. Rev. Lett. **69**, 612 (1992).